Structure, Volume *21*

Supplemental Information

Structural Basis of a Rationally Rewired Protein-Protein Interface Critical to Bacterial Signaling

Anna I. Podgornaia, Patricia Casino, Alberto Marina, and Michael T. Laub

Inventory of Supplemental Information

Supplemental Text

Differential contacts in the rewired functional complex are largely dispensable

To test whether new interactions between the CA domain and RR* in the HK*-RR* complex affect phosphotrasfer, we made mutations at several positions in HK and HK*, introducing either smaller or bulkier residues to try and disrupt the newly observed contacts. For the two mutations in the kinase, S346Y and H347G, there were no significant effects on phosphotransfer or dephosphorylation kinetics (Fig. S3A-B). Two mutants in RR468, D60G and D60E, significantly slowed the rate of dephosphorylation but affected both wild type and mutant HK853 similarly (Fig. S3). As none of the mutations made affected only the HK*-RR* complex, we conclude that these new contacts observed in the HK*-RR* structure are likely not critical to the activity of HK853*.

In contrast, the HK-RR* complex has lost all contacts with the CA domain but maintains three DHp-RR α1 interactions (A268-P13, Y272-M17 and F291-M17) conserved in the three complexes. The HK-RR* complex also shows new interactions between HK α1 with RR α1 (T287-F20 and E290-F20) and with β5 strand (E282-S110 and E282-Q111). As a result, RR468* has recognized a similar region to anchor to the kinase but the lack of complementarity with the kinase has forced the RR to slide around the DHp domain.

Although the key specificity residues pack against each other in both HK-RR and HK*-RR* complexes, certain intermolecular interactions involving the base of the DHp domain and receiver domain are lost in HK*-RR* due to the relative rotation of the RR*. We made mutations at sites outside the rewired specificity residues to test the importance of these lost interactions (Fig. S1). The mutations K16A and K24A in the response regulator and S279G, S279L, and E290Y in the kinase had no effect on phosphotransfer kinetics of either the HK-RR or the HK*-

RR* complexes (Fig. S3C). Mutation L283G, which is located in the α1-α2 linker of the histidine kinase, led to a minor decrease in phosphatase activity for both HK-RR and HK*-RR* complexes. Thus, the residues at the bottom of the DHp domain are in contact in the HK-RR complex, but are not critical for the interaction of TM853 and RR468. In sum, the structural differences between the HK-RR and HK*-RR* structures do not result in significant differences in phosphotransfer or dephosphorylation by the two protein complexes. Despite having a new set of specificity residues, HK*-RR* is functionally and structurally very similar to HK-RR.

Figure S1

A

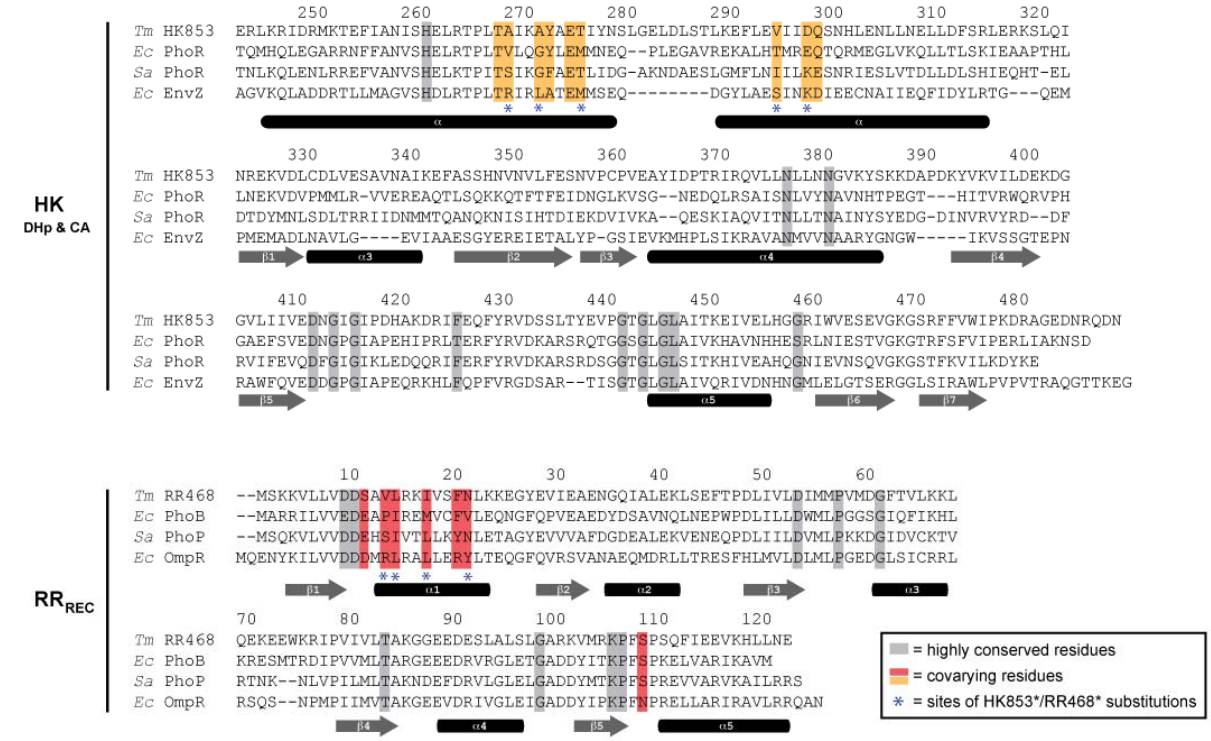
HK
DHp & CA
RR$_{REC}$
Tm HK853
Ec PhoR
Sa PhoR
Ec EnvZ
Tm RR468
Ec PhoB
Sa PhoP
Ec OmpR
= highly conserved residues
= covarying residues
= sites of HK853*/RR468* substitutions

B

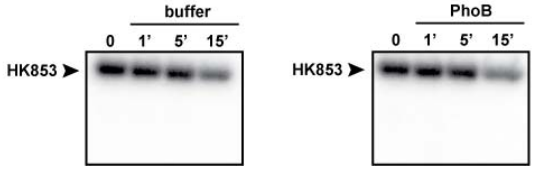
buffer
PhoB
0
1'
5'
15'
HK853

Figure S2

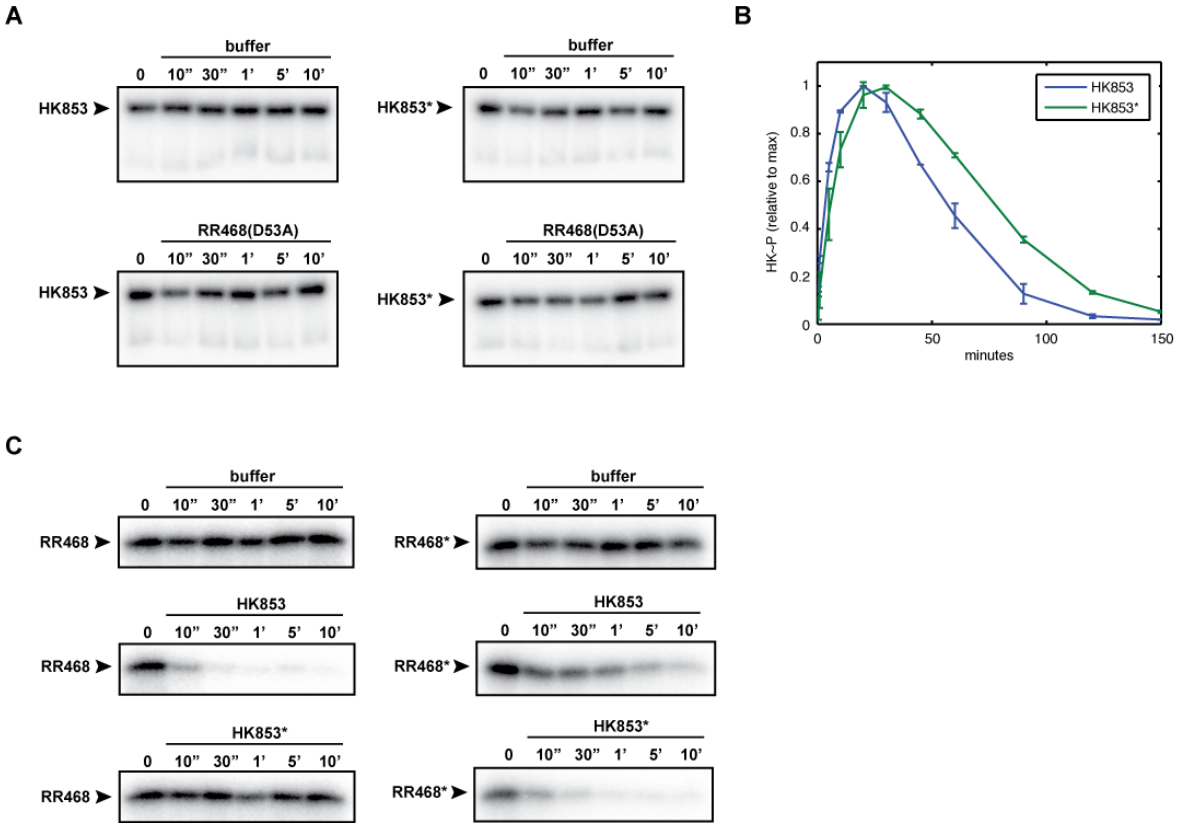
A
buffer
0 10" 30" 1' 5' 10'
HK853
HK853*
RR468(D53A)
B
HK853
HK853*
HK-P (relative to max)
minutes
C
RR468
RR468*
HK853
HK853*

Figure S3

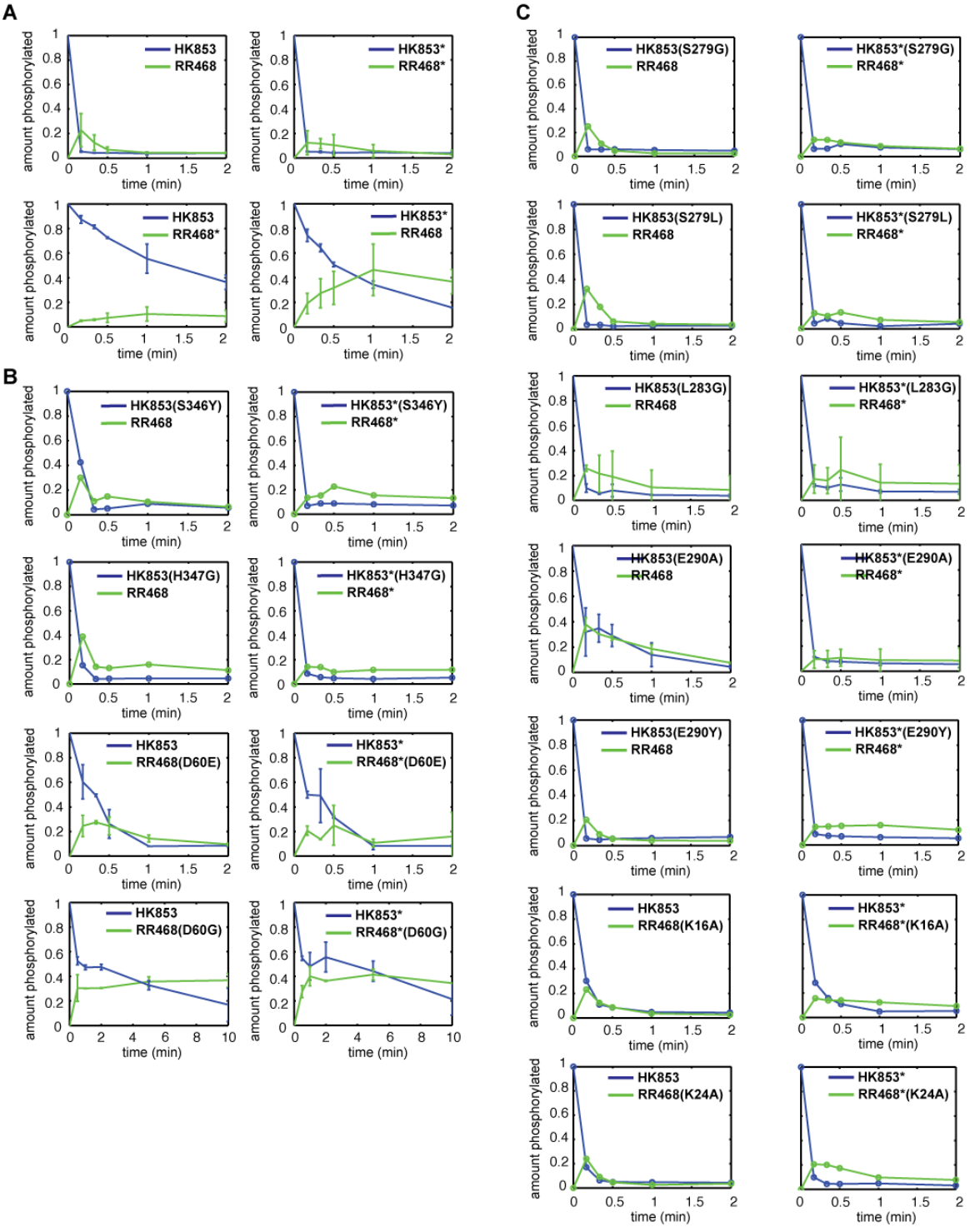
A
HK853
RR468
HK853*
RR468*
HK853
RR468*
HK853*
RR468
B
HK853(S346Y)
RR468
HK853*(S346Y)
RR468*
HK853(H347G)
RR468
HK853*(H347G)
RR468*
HK853
RR468(D60E)
HK853*
RR468*(D60E)
HK853
RR468(D60G)
HK853*
RR468*(D60G)
C
HK853(S279G)
RR468
HK853*(S279G)
RR468*
HK853(S279L)
RR468
HK853*(S279L)
RR468*
HK853(L283G)
RR468
HK853*(L283G)
RR468*
HK853(E290A)
RR468
HK853*(E290A)
RR468*
HK853(E290Y)
RR468
HK853*(E290Y)
RR468*
HK853
RR468(K16A)
HK853*
RR468*(K16A)
HK853
RR468(K24A)
HK853*
RR468*(K24A)
amount phosphorylated
time (min)

Figure S4

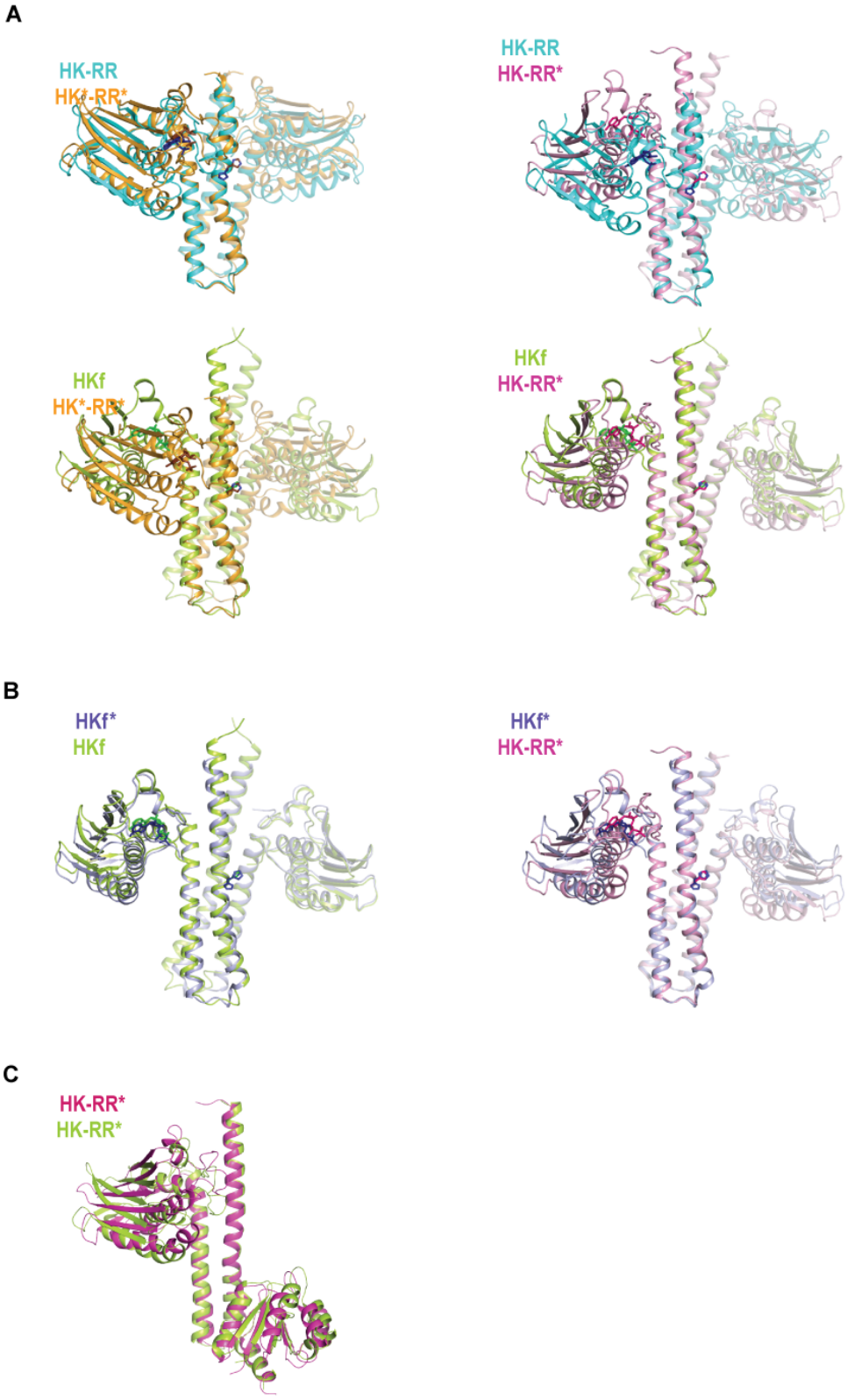
A
HK-RR
HK*-RR*
HK-RR
HK-RR*
HKf
HK*-RR*
HKf
HK-RR*
B
HKf*
HKf
HKf*
HK-RR*
C
HK-RR*
HK-RR*

Figure S5

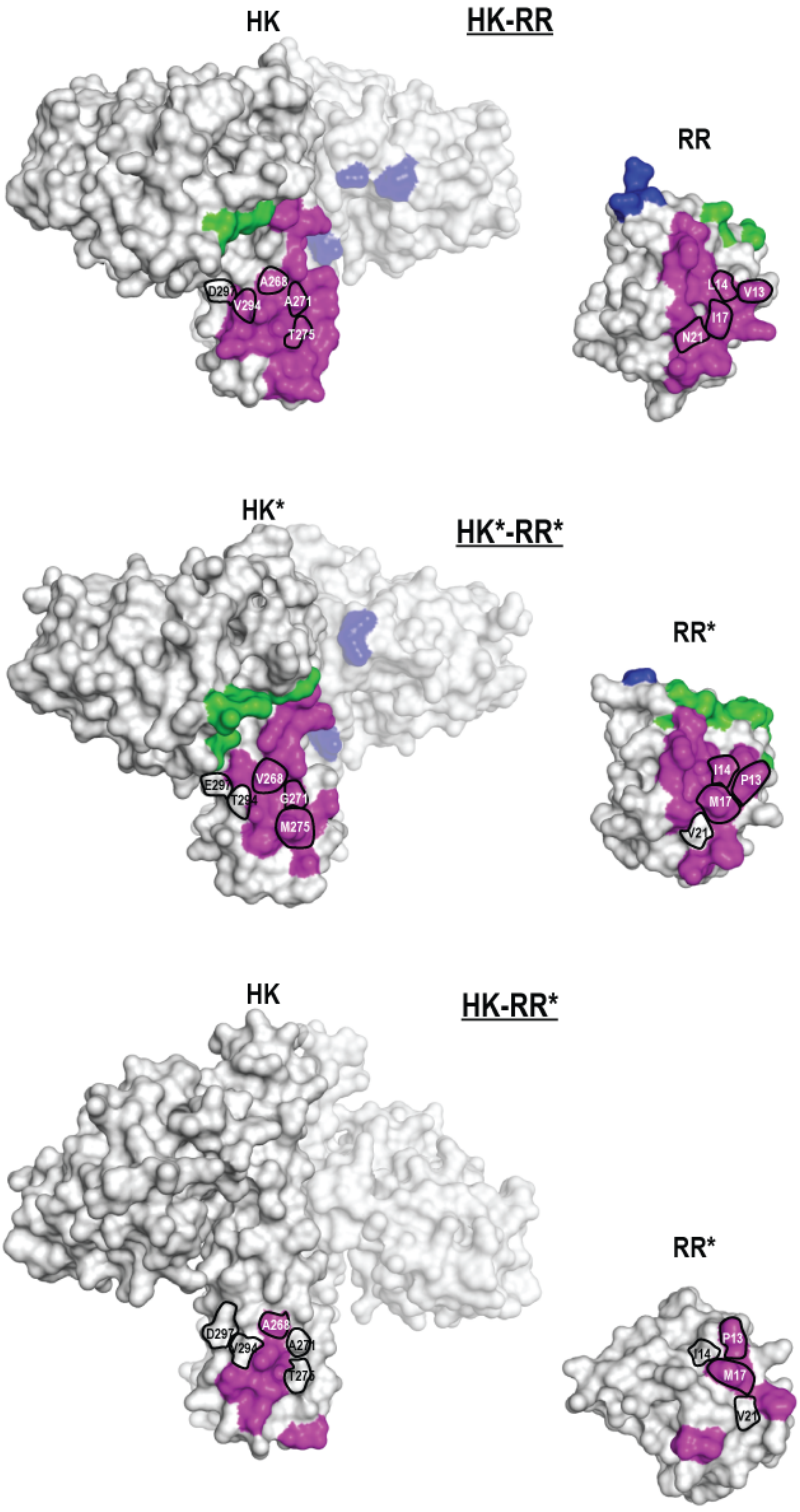
HK
HK-RR
RR
D297
A268
V294
A271
T275
L16
V13
I17
N21
HK*
HK*-RR*
RR*
E297
V268
T294
G271
M275
I14
P13
M17
V21
HK
HK-RR*
RR*
D297
A268
V294
A271
T275
P13
I14
M17
V21

Figure S6

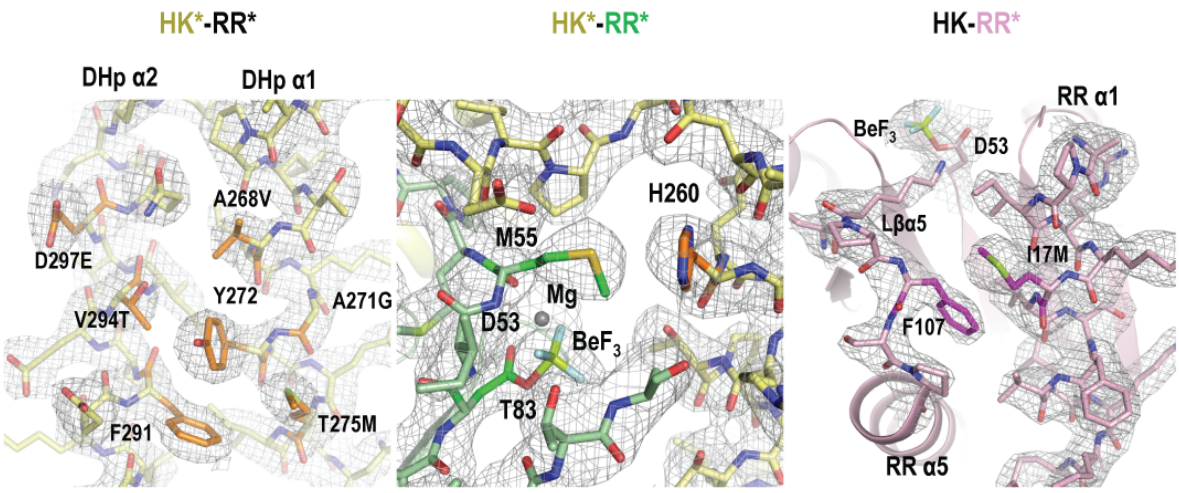
HK*-RR*
HK*-RR*
HK-RR*
DHp α2
DHp α1
A268V
D297E
Y272
A271G
V294T
F291
T275M
H260
M55
Mg
D53
BeF3
T83
BeF3
D53
RR α1
Lβα5
I17M
F107
RR α5

Supplemental Figure Legends

Figure S1, related to Figure 1. Specificity residues in two-component signaling proteins. (A) Multiple sequence alignment of four histidine kinases (DHp and CA domains) and their cognate response regulators (receiver domain only), with specificity residues and highly conserved residues highlighted according to the legend. Species abbreviations as in Figure 1 in main text. (B) Phosphorylated HK853 incubated with PhoB as in Figure 1C, but with buffer control shown for comparison.

Figure S2, related to Figure 2. Kinase and regulator dephosphorylation. (A) Time courses illustrating the stability of autophosphorylated HK853 and HK853* at 4°C. Experiments were performed as in Figure 2. (B) Time course of HK853 and HK853* autophosphorylation at room temperature, starting immediately after the addition of [^{32}P-γ] ATP to 5 μM kinase. Quantified autophosphorylation intensity is shown as percentage of max for each kinase. Error bars show ± SD of two experiments. (C) Phosphatase experiments with RR468 and RR468*. The regulators were phosphorylated using [^{32}P] acetyl-phosphate and incubated with buffer, HK853, or HK853* at 4°C. We used 5 μM of each protein (regulator and kinase) in the RR468 experiments and 10 μM of each protein in the RR468* experiments.

Figure S3, related to Figure 2. Phosphotransfer time-courses. Each histidine kinase construct was autophosphorylated with [^{32}P-γ]ATP and then incubated with the response regulator indicated at 4 °C. Samples were taken at the time points indicated and phosphotransfer assessed by SDS-PAGE and phosphorimaging. Bands corresponding to phosphorylated kinase (blue points) and regulator (green points) were quantified and normalized by the initial amount of autophosphorylated kinase. (A) Wild-type and rewired HK853 and RR468 (also see Fig. 2A-B). (B-C) HK853 and HK853* harboring mutations at (B) the interface between the CA domain and

the response regulator or (C) the interface between the DHp stem and the response regulator (see Supplemental Text). Where shown, error bars represent ± SD of two experiments.

Figure S4, related to Figures 3-6. Superposition of free and complex structures. (A) Top row: superposition of the HK853 component of HK-RR (cyan; PDB:3DGE) with the corresponding component of HK*-RR* (orange) and HK-RR* (magenta). Bottom row: free HK853, HKf, (yellow-green; PDB:2C2A) superposed with the corresponding component of HK*-RR* (orange) and HK-RR* (magenta). (B) Superposition of HKf (yellow-green) with HKf* (blue) and with HK-RR* (magenta). The phosphorylatable His260, as well as the ADP ligand, are shown as sticks in similar color to the cartoon representation of the structure from which they are extracted. (C) Superimposition of the individual HK-RR complexes (green and magenta) present in the asymmetric unit for the HK-RR* structure.

Figure S5, related to Figures 3-6. Surface of interaction in the HK-RR, HK*-RR* and HK-RR* complexes. Surface representation of the three complexes in white, showing a homodimer HK, with one subunit transparent, and one RR molecule separated from the complex and rotated 180° with respect to the HK for visualization purposes. Interactions between the RR and the DHp domain are colored magenta; interactions between the RR and the CA domain are colored green; interactions between the RR and the other subunit of the HK are colored blue. Residues subjected to mutagenesis in the HK are indicated by thick black lines, labeled in white if they interact in the complex and in black if they do not.

Figure S6, related to Figures 3-6. Quality of the electron density maps. The electron density from $2F_o$-F_c maps contoured at 1.0 σ are shown around the complex interface (left), the active center of the HK*-RR* complex (center) and the RR468* contact interface of the HK-RR* complex (right). Notice that the interface views (left and right) are shown in the same orientation

as in Figure 5. More relevant side chains and structural elements are labeled and colored in a darker hue.

Table S1, relates to Figures 3-6. List of intermolecular contacts in the HK-RR, HK*-RR*, and HK-RR* complexes

HK-RR	HK*-RR*	HK-RR*
H260-M55 (H)	H260-K85 (H)	
	H260-A84 (H)	
R263-K105 (P)	R263-K105 (P)	
R263-A84 (H)	R263-A84 (H)	
	T264-S11 (H)	
L266-P106 (H)		
T267-P106 (P)	T267-P106 (H)	
T267-L14 (H)	T267-I14 (H)	
T267-F107 (H)	T267-F107 (H)	
	T267-K105 (H)	
A268-V13 (H)	V268-P13 (H)	A268-P13 (H)
	V268-I14 (H)	
K270-P106 (H)		
K270-F107 (H)		
A271-I17 (H)		
A271-P109 (H)	G271-P109 (H)	
Y272-V13 (P)		
Y272-I17 (H)	Y272-M17 (P)	Y272-M17 (P)
E274-S108 (P)	E274-S108 (P)	
E274-P109 (H)	E274-P109 (H)	
T275-N21 (P)		
T275-I17 (H)	M275-M17 (H)	
T275-F20 (H)	M275-F20 (H)	
N278-K24 (P)		
S279-F20 (H)		
S279-K24 (P)	S279-K24 (P)	
E282-K24 (H)		E282-Q111 (P)
		E282-S110 (P)
L283-F20 (H)		
		T287-F20 (H)
E290-K16 (SB)		E290-F20 (H)
F291-K16 (H)		
F291-I17 (H)		F291-M17 (H)
F291-F20 (H)	F291-F20 (H)	
V294-V13 (H)		
E303-P106 (H)	E303-P106 (H)	
R314-E89 (P)		
R314-G87 (H)		
	R317-E89 (P)	
Q321-E88 (P)		
	S346-E33 (H)	
	H347-P57 (H)	
K387-P57 (H)	K387-M59 (H)	
	K387-Q36 (P)	
	K387-V58 (H)	
	D388-Q36 (P)	
E438-P57 (H)	E438-M56 (P)	
E438-M55 (H)	E438-M55 (H)	
	E438-K85 (SB)	
	P440-M56 (H)	

Type of interactions: (H) Hydrophobic, (P) Polar and (SB) Salt bridge.

Areas of interaction: DHp in magenta, CA in green and with the other subunit in blue.

Table S2, relates to Experimental Procedures. Mutagenesis primers

Primer	Sequence (5' → 3')
HK853(A268V, A271G, T275M)	ACGCCTTTAACGGTCATAAAAGGTTATGCGGAAATGATTTACAACAGT
HK853(V294T, D297E)	GGAGTTCCTCGAGACGATAATAGAGCAAAGCAACCACCTCG
HK853(A268V)	GCTCAGAACGCCTTTAACGGTCATAAAAGCTTATGC
HK853(A271G)	CGCCTTTAACGGCCATAAAAGGTTATGCGGAAAC
HK853(T275M)	GCCATAAAAGCTTATGCGGAAATGATTTACAACAGTCTGGGAG
HK853(M275T) on (A268V, A271G, T275M)	GGTTATGCGGAAACAATTTACAACAGTCTGGGAGAACTGG
HK853(V268A) on (A268V, A271G, T275M)	CAGAACGCCTTTAACGGCCATAAAAGGTTATGCG
HK853(G271A) on (A268V, A271G, T275M)	CCTTTAACGGTCATAAAAGCTTATGCGGAAATGATTTACAAC
HK853(L283G)	CAGTCTGGGAGAAGGGGATCTCAGCACCCTC
HK853(E290A)	GCACCCTCAAGGCGTTCCTCGAGGTG
HK853(E290A) on (V294T)	GCACCCTCAAGGCGTTCCTCGAGACG
HK853(S346Y)	GATCAAAGAATTTGCTTCATATCACAACGTGAATGTTCTCTTTG
HK853(H347G)	GATCAAAGAATTTGCTTCATCTGGCAACGTGAATGTTCTCTTTG
HK853(S279G)	GGAAACAATTTACAACGGTCTGGGAGAACTGGATC
HK853(S279L)	GCGGAAACAATTTACAACCTTCTGGGAGAACTGGATCTC
HK853(E290Y)	GGATCTCAGCACCCTCAAGTACTTCCTCGAGGTG
HK853(V294L)	CAAGGAGTTCCTCGAGCTGATAATAGATCAAAGCAAC
HK853(S279G) on (A268V, A271G, T275M, V294T, D297E)	GGAAATGATTTACAACGGTCTGGGAGAACTGGATC
HK853(S279L) on (A268V, A271G, T275M, V294T, D297E)	GCGGAAATGATTTACAACCTTCTGGGAGAACTGGATCTC
HK853(E290Y) on (A268V, A271G, T275M, V294T, D297E)	GGATCTCAGCACCCTCAAGTACTTCCTCGAGACG
HK853(V294L) on (A268V, A271G, T275M, V294T, D297E)	CTCAAGGAGTTCCTCGAGCTGATAATAGAGCAAAGCAAC
RR468(V13P, L14I)	GTTGATGACTCGGCACCTATCAGAAAAATCGTTTC
RR468(I17M, N21V) on (V13P, L14I)	GGCACCTATCAGAAAAATGGTTTCTTTCGTTCTGAAAAAAGAAGG
RR468(D53A)	CTGATAGTTCTCGCCATAATGATGCCCGTG
RR468(V13P)	CTCGTTGATGACTCGGCGCCTCTGAGAAAAATCGTTTC
RR468(L14I)	CTCGTTGATGACTCGGCGGTTATCAGAAAAATCGTTTCTTTC
RR468(I17M)	CTCGGCGGTTCTGAGAAAAATGGTTTCTTTCAATCTG
RR468(N21V)	CGGTTCTGAGAAAAATCGTTTCTTTCGTTCTGAAAAAAGAAGGTTACG
RR468(I17M) on RR468(N21V)	CTCGGCGGTTCTGAGAAAAATGGTTTCTTTCGTTCTG
RR468(V13P, I17M)	GTTGATGACTCGGCGCCTCTGAGAAAAATGGTTTCTTTCAATCTG
RR468(I17M) on (L14I)	GACTCGGCGGTTATCAGAAAAATGGTTTCTTTCAATCTG
RR468(V21N) on (V13P, L14I, I17M, N21V)	GCACCTATCAGAAAAATGGTTTCTTTCAATCTGAAAAAAGAAGGTTACG
RR468(I14L) on (V13P, L14I, I17M, N21V)	GTTGATGACTCGGCACCTCTGAGAAAAATGGTTTCTTTCG
RR468(P13V) on (V13P, L14I, I17M, N21V)	CTCGTTGATGACTCGGCAGTTATCAGAAAAATGGTTTCTTTCG
RR468(D60E)	GATGCCCGTGATGGAAGGATTCACCGTG
RR468(D60G)	GATGCCCGTGATGGGTGGATTCACCGTG
RR468(K16A)	GACTCGGCGGTTCTGAGAGCAATCGTTTCTTTCAATCTG
RR468(K24A)	CGTTTCTTTCAATCTGAAAGCAGAAGGTTACGAAGTGATAGAAGC
RR468(K16A) on (V13P, L14I, I17M, N21V)	GACTCGGCACCTATCAGAGCAATGGTTTCTTTCGTTCTG
RR468(K24A) on (V13P, L14I, I17M, N21V)	GGTTTCTTTCGTTCTGAAAGCAGAAGGTTACGAAGTGATAGAAGC
PhoB(M17I, V21N)	GCTCCAATTCGCGAAATCGTCTGCTTCAACCTCGAACAAAATGGCTTTC
PhoB(P13V, I14L) on (M17I, V21N)	GGTCGTAGAAGATGAAGCTGTACTTCGCGAAATCGTCTGCTTC

Table S3, relates to Experimental Procedures. Cloning primers

Primer	Sequence (5' → 3')
HK853-pET24b (insert)-FW	AGGAGATATACCATGGAAAATGTGACAGAATCAAAAGA
-RV	CTTTTGGGATCCACACAAAGA
HK853-pET24b (vector)-FW	TGTGGATCCCAAAAGACCGT
-RV	CATGGTATATCTCCTTCTTAAAG
RR468-pET22b (insert)-FW	GAAGGAGATATACATATGTCTAAAAAAGTTCTTCTCGTT
-RV	GTGGTGGTGCTCGAGTCATTCATTTAATAGATGCTTCAC
RR468-pET22b (vector)-FW	CTCGAGCACCACCACCAC
-RV	ATGTATATCTCCTTCTTAAAGTTA